

SLOW EXTRACTION FROM SIS-100 AT HIGH BEAM INTENSITY

S. Sorge*, GSI, Darmstadt, Germany

INTRODUCTION

The heavy ion synchrotron SIS-100 will play a key role within the future FAIR project underway at GSI. Although this synchrotron is optimised for fast extraction, also slow extraction will be used.

A major requirement to provide high-intensity beams, particularly, of the reference heavy ion U^{28+} . Uncontrolled beam loss within high-intensity operation can lead to irradiation of the device and degradation of the vacuum resulting in a reduction of the beam life time. During slow extraction, particles can become lost due to collisions with the blade of the electro-static (ES) septum, where they are scattered out of the beam. Furthermore, the particle collisions can damage or destroy the ES septum blade.

Slow extraction from SIS-100 is based on the excitation of the 3rd order resonance given by $52 = 3\nu_x$ by means of 11 resonant sextupoles. During slow extraction, the particles leave the phase space area occupied by the beam along separatrices. The spread in the particle momenta generating a tune spread causes an effective broadening of the separatrices resulting in an increase of the cross section for particle collisions with the ES septum. A reduction of this tune spread will be achieved by the correction of the horizontal chromaticity ξ .

The extraction process can be influenced by additional, undesired non-linearities in the lattice arising from errors in magnets and space charge fields. In the present study, systematic errors in bending magnets and quadrupoles as well as the space charge of the ion beam have been included in a particle tracking model based on the MAD-X code. The space charge has been introduced as frozen space charge. Although the maximum number of U^{28+} ions is $5.0 \cdot 10^{11}$, simulations with space charge according to an ion number up to $N_{ion} = 5.0 \cdot 10^{12}$ have been performed in order to investigate the effect of very large space charge fields. Furthermore, the lowest extraction energy $E = 400$ MeV has been used.

First results are presented in this work, where, up to now, the simulations were restricted to a few thousand turns and test particles. Calculations concerning longer time intervals and using larger test particle ensembles will be done later.

SETTINGS AND PARAMETERS

Chromatic Sextupoles

A reduction of the dependence of the separatrices to reduce beam loss due to particle collisions with the ES septum blade can be achieved by a correction for the chromaticity [2].

Table 1: SIS-100 Parameters as Proposed in the Technical Design Report [1]. The horizontal position of the ES septum blade are negative although it is located at the outer side of the ring because the direction of beam motion in SIS-100 is counterclockwise so that the x axis points to the centre of the ring.

Circumference, C	1083.6 m
Reference ion	U^{28+}
Maximum ion number, $N_{ion,max}$	$5.0 \cdot 10^{11}$
Working point, ν_x, ν_y	17.31, 17.8
Harmonic number of the resonance, n	52
Hor. Twiss functions at ES septum start: β_x α_x	16.126 m 1.23
Number of sextupoles for resonance excitation, M_{rsext} chromaticity correction, M_{csext}	11 48
Sextupole amplitude, $k_{2,a}L$, Equation (1) Standard settings Modified settings Chromatic sextupoles' strength, $k_{2,c}L$ Harmonic number h , Equation (1)	0.15 m^{-2} 0.7 m^{-2} -0.41 m^{-2} 4
Hor. ES septum blade position, x_{sep} Tilt angle of ES septum blade, x'_{sep}	-41 mm 1.3 mrad
RMS momentum spread, δ_{rms}	$5 \cdot 10^{-4}$

For that purpose, 48 chromatic sextupole will be installed in SIS-100. It turned out that the vertical dynamic aperture is strongly decreased if the chromaticity is corrected to a degree that the Hardt condition is totally fulfilled [3]. Therefore, in the present scheme only a partial correction of the chromaticity is foreseen. The natural chromaticity is $(\xi_{nat,x}, \xi_{nat,y}) = (-1.17, -1.16)$, after correction it is $(\xi_{corr,x}, \xi_{corr,y}) = (-0.29, -2.23)$. That will be performed using a scheme where all 48 chromatic sextupoles have the focussing strength $k_{2,c}L = -0.408 \text{ m}^{-2}$ [4], see Figure 2.8-19 in in [1]. In doing so, a large maximum strength is avoided which could drive additional resonances.

Resonant Sextupoles

Slow extraction from SIS-100 will be done using the 3rd order resonance given by $52 = 3\nu_x$ excited by 11 resonant sextupoles. They are symmetrically located in the ring, where there are two sextupoles in each section except for the section used for beam transfer from SIS-100 to the next synchrotron SIS-300. The focussing strengths of the

*S.Sorge@gsi.de

resonant sextupoles are given by [4]

$$k_{2,m} = k_{2,a} \sin\left(\frac{2\pi s_m}{C} + \phi_0\right), \quad (1)$$

where s_m are the locations of the sextupoles, C is the circumference of the ring, and $h = 4$ is the harmonic number. $k_{2,a}$ is the sextupole “amplitude” defining the maximum possible focussing strength. ϕ_0 is a phase which determines the orientation of the triangular stable area in horizontal phase space.

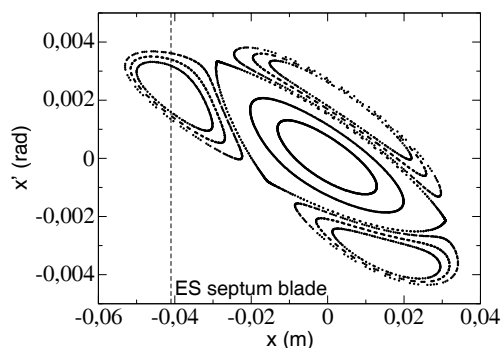


Figure 1: Stable particle trajectories in horizontal phase space for a lattice with standard sextupole settings.

The actual standard scheme for the focussing strengths proposed in [1, 5] uses sextupoles with $k_{2,a}L = 0.15 \text{ m}^{-2}$. So, the resonant sextupoles are weaker than the those for chromaticity correction. A consequence is the formation of stable islands in horizontal phase space which include the position of the ES septum blade, see Figure 1. Particles will not reach the islands, if they are extracted sufficiently fast. Indeed, it could be shown by means of multi-particle tracking calculations that slow extraction occurs with a particle loss rate below 10 % because the particles are sufficiently fast extracted so that only a few particles reach the islands [6].

To circumvent such uncertainties, a modified sextupole scheme with $k_{2,a}L = 0.7$ has been introduced [6]. Using that, particle loss below 5 % has been obtained in multi-particle tracking calculations.

In this study, results obtained with both settings are presented because it is not finally decided, yet, which settings will be used.

KO Exciter

In SIS-100, KO extraction is foreseen as the standard procedure for slow extraction. To regard that in the present study, an element providing a transverse beam excitation by means of a sinusoidal momentum kick has been implemented in the thin lens tracking tool of MAD-X.

In most of the simulations, the simulation interval was restricted to 5000 turns. The corresponding time interval at $E = 400 \text{ MeV/u}$ is about $t = 0.03 \text{ s}$. In reality, the extraction process will have a duration of about 1 s corresponding to ≈ 150000 turns. As a consequence, the

maximum deflection angle of the KO exciter in the simulations has been chosen to be much larger than it would be possible in reality. The KO exciter was represented by 26 sinusoidal kickers with an amplitude deflection angle $\Delta x'_a = 0.002 \text{ mrad}$. The resulting maximum deflecting angle is $\Delta x'_{max} = 26 \cdot 0.002 \text{ mrad} = 0.052 \text{ mrad}$, what is about one order of magnitude larger than the probable realistic value. The frequencies of the 26 kicks are equidistantly set in a frequency interval which corresponds to the interval of the fractional tune $\nu_{frac} \in [0.3, 0.34]$ to cover the fractional tune of all particles as well as that of the resonance.

Magnet Errors

To include the systematic field errors of the bending magnets and quadrupoles, the representation of the magnetic field by multipoles components,

$$B_y + iB_x = B\rho \sum_{n=0}^{\infty} (k_n + ij_n) \frac{(x + iy)^n}{n!}, \quad (2)$$

has been used. k_n and j_n are normal and skewed multipole components, respectively, which were theoretically determined [7, 8]. Separate multipole components for the body and the edge of each magnet type up to $n = 16$ have been taken into account in this study.

Inclusion of the Space Charge

In the calculations, the space charge has been introduced in the SIS-100 lattice given as a MAD-X script as non-linear transverse momentum kicks using the BEAMBEAM element. Here, a Gaussian beam was assumed. The procedure to implement the space charge kicks in the lattice consists of three steps [9]. At the beginning, markers are put at the locations foreseen for the space charge kicks. After

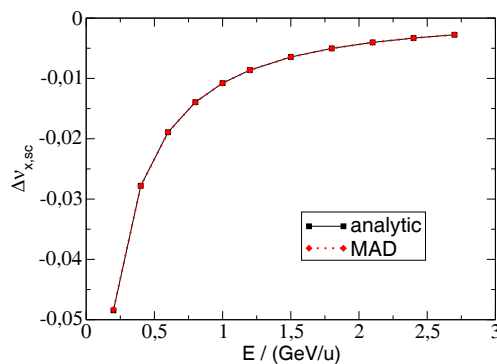


Figure 2: Horizontal Laslett tune of a beam of $5.0 \cdot 10^{11} \text{ U}^{28}$ ions determined from analytical formula vs. MAD-X simulation using dynap module. The emittances were chosen according to $\epsilon_{rms,x} = 8.75 \text{ mm mrad}$ and $\epsilon_{rms,y} = 3.75 \text{ mm mrad}$ at injection energy, $E = 0.2 \text{ GeV/u}$, and the assumption of conservation of the normalised emittances.

that, the beta function at these locations is determined and stored. Finally, the markers are replaced with space charge kicks, where their RMS width is matched to the initial RMS beam width given by $\sigma_z = \sqrt{\beta_z \epsilon_{rms,z}}$, $z = x, y$. The number of space charge kicks was 48 placed at equidistant positions in the lattice. The phase advance between was about $2.0\pi \cdot \nu_y / 48 = 2\pi \cdot 0.37$. The influence of the number of space charge kicks needs still to be studied.

Nevertheless, a very good agreement between the Laslett tune shift determined with MAD-X and that given by the analytic formula for a Gaussian beam [10],

$$\Delta\nu_{sc,z} = -\frac{N_{ion}r_0}{2\pi\beta^2\gamma^3\sqrt{\epsilon_{rms,z}}(\sqrt{\epsilon_{rms,x}} + \sqrt{\epsilon_{rms,y}})} \quad (3)$$

could be achieved, where $r_0 = q^2/(4\pi\epsilon_0m_0c^2)$ is the classical radius of an ion of rest mass m_0 and charge q . The Laslett tune shift for U^{28+} and $N_{ion} = 5.0 \cdot 10^{11}$ is shown as a function of the energy in Figure 2.

PARTICLE LOSS

The first step was to study slow extraction perturbed only by space charge.

For both sextupole schemes, no dramatic increase of beam loss due to space charge according has been observed, as long as an ion number $N_{ion} \leq 10^{12}$ was assumed. If weak sextupoles according to the standard sextupole settings were used in the simulations, an increase of space charge even led to a reduction of particle loss, as one can see in Figure 3. In case of using sextupoles according to the modified scheme, a slight increase in beam loss appeared.

A strong increase in beam loss was observed only for ion numbers far above $N_{ion} = 10^{12}$. On the other hand, the inclusion of space charge led to a strong deformation of the horizontal phase space area. So, for $N_{ion} = 5.0 \cdot 10^{12}$, the horizontal stable phase area no longer has a triangular shape which indicates that the influence of the resonant sextupoles is strongly reduced. That resulted in a strong decrease of the number of extracted test particles to about 1 % of the initial test particle number. As one can see in Figure 4, all dots of the black graphs remain in the beam, where 100 test particles had been started for each graph in this figure.

The magnet errors were found to affect the beam loss only if also space charge was present. The beam loss found in the simulations is shown in Table 2.

Nevertheless, all results have, possibly, a large error due to bad statistics as a consequence of a small number of extracted test particles. Hence, further studies with larger numbers of test particles and turns are necessary.

SUMMARY

For the present study, systematic magnet errors as well as frozen space charge have been taken into account in a

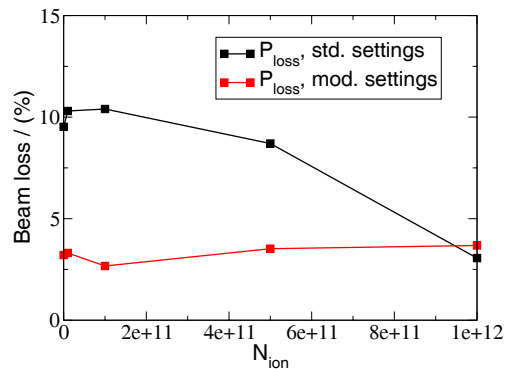


Figure 3: Particle loss for both sextupole schemes and vertical tune affected by space charge as a function of the ion number N_{ion} . The vertical black solid line denotes the tune $\nu_y = 17.5$.

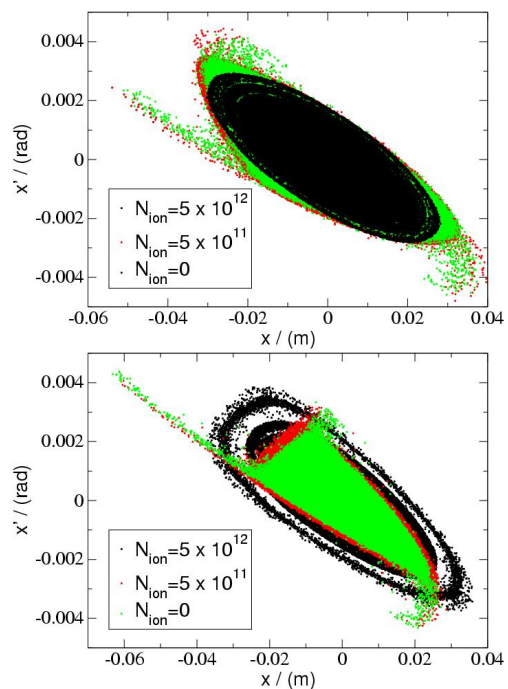


Figure 4: Horizontal phase space plot of the particles' coordinates depending on the ion number for standard sextupole settings (graph above) and modified sextupole settings (graph below).

particle tracking model. This model has been used to simulate slow extraction from SIS-100 in order to estimate particle loss due to particle collisions at the ES septum blade affected by both these effects. In the simulations, two schemes for the focussing strengths of the resonant sextupoles were applied, the standard scheme with weak resonant sextupoles and a modified scheme with strong resonant sextupoles. For both schemes, the inclusion only of the space charge led to a significant increase of beam loss, only if the number of ions in the beam generating the space charge field is much larger than it will be in reality. For

Table 2: Particle Loss Affected by Space Charge and Magnet Errors

(a) Standard sextupoles settings

	$N_{ion} = 0$	$N_{ion} = 5.0 \cdot 10^{11}$
without magnet errors	10.0 %	8.7 %
with magnet errors	10.0 %	12.7 %

(b) Modified sextupoles settings

	$N_{ion} = 0$	$N_{ion} = 5.0 \cdot 10^{11}$
without magnet errors	3.2 %	3.5 %
with magnet errors	3.2 %	4.0 %

realistic space charge fields, the beam loss was systematically increased by space charge only if also the magnet errors were taken into account.

Generally, the simulations showed that both, space charge as well as magnet errors do not cause a dramatic increase in beam loss.

On the other hand, the number of test particles in the simulations was not very large. Furthermore, the number of extracted test particles was, in particular if the standard sextupole settings were applied, even smaller, and it was further reduced if space charge was taken into account. For those reasons, the particle loss obtained has, possibly, a large error. Therefore, further simulations with more particles and during longer time intervals are necessary to verify the results.

REFERENCES

- [1] FAIR Technical Design Report – SIS100, GSI Darmstadt 2008.
- [2] W. Hardt, “Ultraslow extraction out of LEAR”, PS/DL/LEAR Note 81-6, $\bar{p}p$ LEAR Note 98, CERN 1981.
- [3] A. Bolshakov, G. Franchetti, and P. Zenkevich, “Effect of nonlinear lattice and chromatic correction system on slow extraction from SIS100”, GSI internal report, GSI Darmstadt 2007.
- [4] N. Pyka, private communication.
- [5] K. Blasche and B. Franczak, “SIS100 Design Review”, GSI internal report, GSI Darmstadt 2007.
- [6] S. Sorge, G. Franchetti, O. Boine-Frankenheim, and A. Bolshakov, “Study on Particle Loss during Slow Extraction from SIS-100”, Proc. of IPAC 2010, Kyoto, Japan.
- [7] P. Akishin, E. Fischer, and P. Schnizer, “3D field calculations for SIS100 dipoles”, GSI, November, 2007.
- [8] V. Kapin and G. Franchetti, GSI-Accelerator-Note 2008-001, GSI, Darmstadt, 2008.
- [9] V. Kapin, private communication.
- [10] A. Hofmann, CERN, “Tune Shifts from Self Fields and Images”, p. 336